JOURNAL OF GEOPHYSICAL RESEARCH, VOL. 112, D10S39, doi:10.1029/2006JD007584, 2007

Chemical composition observed over the mid-Atlantic and the detection of pollution signatures far from source regions

A. C. Lewis,[1] M. J. Evans,[2] J. Methven,[3] N. Watson,[1] J. D. Lee,[1] J. R. Hopkins,[1] R. M. Purvis,[1,4] S. R. Arnold,[2] J. B. McQuaid,[2] L. K. Whalley,[2] M. J. Pilling,[2] D. E. Heard,[2] P. S. Monks,[5] A. E. Parker,[5] C. E. Reeves,[6] D. E. Oram,[6] G. Mills,[6] B. J. Bandy,[6] D. Stewart,[6] H. Coe,[7] P. Williams,[7] and J. Crosier[7]

Received 31 May 2006; revised 21 September 2006; accepted 17 November 2006; published 13 February 2007.

[1] The atmospheric composition of the central North Atlantic region has been sampled using the FAAM BAe146 instrumented aircraft during the Intercontinental Transport of Ozone and Precursors (ITOP) campaign, part of the wider International Consortium for Atmospheric Research on Transport and Transformation (ICARTT). This paper presents an overview of the ITOP campaign. Between late July and early August 2004, twelve flights comprising 72 hours of measurement were made in a region from approximately 20 to 40°W and 33 to 47°N centered on Faial Island, Azores, ranging in altitude from 50 to 9000 m. The vertical profiles of O_3 and CO are consistent with previous observations made in this region during 1997 and our knowledge of the seasonal cycles within the region. A cluster analysis technique is used to partition the data set into air mass types with distinct chemical signatures. Six clusters provide a suitable balance between cluster generality and specificity. The clusters are labeled as biomass burning, low level outflow, upper level outflow, moist lower troposphere, marine and upper troposphere. During this summer, boreal forest fire emissions from Alaska and northern Canada were found to provide a major perturbation of tropospheric composition in CO, PAN, organic compounds and aerosol. Anthropogenic influenced air from the continental boundary layer of the USA was clearly observed running above the marine boundary layer right across the mid-Atlantic, retaining high pollution levels in VOCs and sulfate aerosol. Upper level outflow events were found to have far lower sulfate aerosol, resulting from washout on ascent, but much higher PAN associated with the colder temperatures. Lagrangian links with flights of other aircraft over the USA and Europe show that such signatures are maintained many days downwind of emission regions. Some other features of the data set are highlighted, including the strong perturbations to many VOCs and OVOCs in this remote region.

Citation: Lewis, A. C., et al. (2007), Chemical composition observed over the mid-Atlantic and the detection of pollution signatures far from source regions, *J. Geophys. Res.*, *112*, D10S39, doi:10.1029/2006JD007584.

1. Introduction

[2] It has become increasingly clear in recent years that surface emissions and resulting photochemical pollution may no longer be considered only in the context of local air quality, but that it has potential to be transported on both regional and continental scales [*Fehsenfeld et al.*, 1996a; *Penkett et al.*, 1998]. The uplift of pollutants from the continental boundary layer to the mid and upper troposphere has been detected in previous experiments and a combination of models and observations indicate that this may occur via large-scale advection [e.g., *Fehsenfeld et al.*, 1996b], deep convection [*Liu et al.*, 2003] and convection embedded within frontal systems [e.g., *Purvis et al.*, 2003]. In the middle and upper troposphere jet streams enable the transport of chemicals on scales of thousands of miles in distinct stratified layers of pollution rich air [e.g., *Stohl and Trickl*, 1999; *Trickl et al.*, 2003]. The long-range transport of primary anthropogenic emissions of NO_x and volatile organic compounds (VOCs) may lead to further downstream increases in free troposphere concentrations of radiatively active species such as ozone and aerosols,

[1]Department of Chemistry, University of York, York, UK.
[2]Institute for Atmospheric Science, School of Earth and Environment, University of Leeds, Leeds, UK.
[3]Department of Meteorology, University of Reading, Reading, UK.
[4]Now at Facility for Airborne Atmospheric Measurements, Cranfield University, Bedford, UK.
[5]Department of Chemistry, University of Leicester, Leicester, UK.
[6]School of Environmental Sciences, University of East Anglia, Norwich, UK.
[7]School of Earth, Atmospheric and Environmental Sciences, University of Manchester, Manchester, UK.

0148-0227/07/2006JD007584$09.00

beyond that of direct boundary layer exchange; as well as influencing free radical chemistry because of processes such as carbonyls photolysis. Future trends in primary and secondary pollutants, and the ability of remote regions of the ocean to buffer against them, must therefore be quantified from both direct export and in situ free tropospheric production perspectives.

[3] Regional and global increases in tropospheric ozone and aerosols are of significance from a climate change viewpoint. In addition, the subsidence of such air many thousands of miles downwind of continental source, may lead to elevated background concentrations reentering the boundary layer. Any such increase in what may be considered the baseline concentration prior to further local or regional production, will have significant impact in determining feasible local air quality targets, and will raise cumulative population and biomass exposure [*Li et al.*, 2002].

[4] Surface observations made at the Mace Head observatory, Ireland, have shown that long-range transport of chemicals can occur from North America at low levels although it is atypical [*Derwent et al.*, 1998; *Methven et al.*, 2001]. In general, low level outflow from USA travels at lower latitudes toward the Azores while outflow that is lofted higher in Warm Conveyor Belts (WCBs) is carried poleward and crosses toward Europe in the middle and upper troposphere and may subsequently be observed above observatories on the European mainland [*Wenig et al.*, 2003]. Observations at Mace Head in summer 2002 [*Heard et al.*, 2005] indicated that significant chemical activity remained in anthropogenic polluted air masses which had undergone low level long-range transport, notably in the form of sequestered nitrogen oxides as organic nitrates and reactive carbon in the form of carbonyl intermediates [*Carpenter et al.*, 2004]. The observation of such reactive oxygenate throughout the troposphere is now fully established [*Wang et al.*, 1998; *Singh et al.*, 2001] and it is becoming better understood that much of their presence may be explained by the in situ and continued formation of species such as acetone and methanol during long-range transport [*Lewis et al.*, 2005] and that this may have a notable influence on localized oxidizing capacity.

[5] The chemical transformation of polluted air masses during intercontinental transport will therefore be via reaction schemes of significantly greater complexity than the traditionally considered low NO_x, CO/CH_4 dominated chemistry of maritime background air. Surface locations however provide only very limited opportunity to study long-range transport events, since such low level outflow is atypical of the pathways in which most polluted air masses are transported across the Atlantic. This therefore requires highly detailed observations to be made from aircraft, if both the rate of primary emission removal and secondary pollutant production are to be ultimately tested by comparison of observation with predictive model. Since the transport of pollution in regions such as the upper troposphere has been seen to be highly stratified with only limited mixing (observed for example during 1997 ACSOE experiments [*Penkett et al.*, 2004] and also by *Methven et al.* [2003] and *Newell et al.* [1999]), the integration of regional sources into the Northern Hemisphere background remains however a key uncertainty. While transport from N. America to Europe is one possible outcome for pollution introduced to the mid latitude free troposphere, large-scale flow into high OH regions in the Tropics, or "storage" in Arctic regions are both alternative fates for such air masses. An overview of previous aircraft observations of long-range chemical transport is given in detail by *Fehsenfeld et al.* [2006].

[6] The Intercontinental Transport of Ozone and Precursors (ITOP) project was formed as a component of the wider International Consortium for Atmospheric Research on Transport and Transformation (ICARTT) consortium project with specific reference to chemical evolution in mid Atlantic regions. Further background details are given by *Fehsenfeld et al.* [2006] which sets out the primary objectives of the experiment.

[7] This paper provides an overview of the key observations made during July/August 2004 by the FAAM (Facility for Airborne Atmospheric Measurements) BAe146 aircraft and places these in context with previous aircraft observations in the same region made in April and September 1997. A summary and description of the major chemical properties of a variety of the encountered air mass types will be made and linked to papers which will study certain features in greater detail.

2. ITOP Experiment

[8] The observational programme was centered on Faial Island (38.58°N, 28.72°W) in the Azores archipelago, with a series of 12 flights comprising 72 hours of measurement made using the FAAM BAe146. The aircraft operated from 50 m over the sea surface, to 9000 m, and spatially between 20–40°W and 33–47°N. A summary of the observing platform details and instruments used for observations from this aircraft is given by *Fehsenfeld et al.* [2006] with appropriate links to published instrument methodologies. The measurement base was close to the Pico NARE observatory and on several flights comparison was made between this long-term site atop Pico Volcano and the aircraft. Details of the longer-term climatology determined from the Pico station are given by D. Helmig et al. (unpublished manuscript, 2006). A significant aim of the ICARTT project as a whole was to resample an air mass on several occasions as it passed across the Atlantic forming the ITCT Lagrangian-2K4 (Intercontinental Transport and Chemical Transformation) activity of IGAC. The exercise could be described as a pseudo-Lagrangian experiment, where a single air mass is followed as it evolves over time; however, because of the scales involved, the resampling was undertaken by different aircraft at different time periods in the evolution. This involved special forecasting techniques to identify target air masses and intercept them on several occasions over periods of up to 10 days, as discussed by *Methven et al.* [2006]. To enable quantitative comparison between observations, a matrix of intercomparison between all aircraft in ICARTT was established. The primary intercomparison for the BAe146 was with the DLR Falcon and NASA DC8 aircraft. Details of this intercomparison can be found in an appendix to *Fehsenfeld et al.* [2006].

[9] The BAe146 aircraft had an endurance of approximately 5 hours 30 min with full science payload and at science speed of 200 knots ($\sim$100 m s^{-1}) resulting (because of limited diversion airfields) in a range limit of around

Table 1. Summary of ITOP-UK Flights With Air Mass Types Sampled and Key Features[a]

Flight	Flight Description	Air Mass Types[b]	Lagr. Case	Date in 2004	Takeoff-Landing Times, UTC
B028	transit from Cranfield, UK, to Faial, Azores (refuel Oporto); Alaskan fire plumes encountered over UK SW approaches	B		12 Jul	0930–2130
B029	NW of Azores, low level outflow from US and interception of Alaskan fire plumes	L, B, MT		15 Jul	0842–1326
B030	south and west of Azores, low level/midlevel polluted features from USA	M, MT		17 Jul	1256–1737
B031	north of Azores to limit of aircraft range into low level outflow.	L, U, MT	1	19 Jul	0904–1405
B032	Alaskan fire plumes intercepted in midtroposphere above Azores	L, B, UT	2	20 Jul	0837–1315
B033	to west of Azores for ENVISAT underpass and low level pollution	L, U, M, MT, UT		22 Jul	0920–1349
B034	outflow from Africa; refuel Santa Maria; reinterception of low level outflow	L, U, M, MT, UT	1	25 Jul	0928–1624
B035	DC8 intercomparison to west of Azores, mainly in clean marine air; upper level outflow	U, M, UT		28 Jul	1157–1632
B036	upper level outflow in WCB from US + Alaskan fire plume at higher T	L, U, B, MT	4	29 Jul	0830–1300
B037	NW of Azores; low level frontal system sampled by P3 +fires +stratospheric influence	L, U, B, MT	5	31 Jul	0830–1315
B038	NE of Azores into low level frontal structure sampled the previous day	L, U, B, MT	5	1 Aug	0744–1244
B039	transit from Faial to Cranfield, UK (refuel Oporto), with DLR Falcon intercomparison	L, U, B, MT		3 Aug	0722–1514

[a]"Lagr Case" refers to the Lagrangian case studies identified by *Methven et al.* [2006].
[b]Air mass types encountered most frequently, as determined by cluster analysis. L, low level outflow; U, upper level outflow; B, biomass burning; M, maritime influence; MT, moist midtroposphere; UT, upper troposphere.

925 km from the Faial base. *Fehsenfeld et al.* [2006] show a summary of individual flight tracks for the ITOP experiment. Most flights obtained at least one full atmospheric profile from 50 m to aircraft ceiling. Table 1 provides a summary of aircraft flights and main features observed including the dominant air mass types encountered. Air mass classification is discussed in later sections of this paper.

[10] Various other papers within this special section describe specific uses of the data collected here. *Methven et al.* [2006] establish that Lagrangian links between aircraft spanning the North Atlantic were successfully achieved during the ICARTT campaign. S. R. Arnold et al. (Statistical inference of OH concentrations and air mass dilution rates from successive observations of nonmethane hydrocarbons in single air masses, submitted to *Journal of Geophysical Research,* 2006, hereinafter referred to as Arnold et al., submitted manuscript, 2006) utilize these experiments to investigate our ability to calculate OH concentrations on the basis of the changes of VOC concentrations between interceptions of air masses. A discussion of the distribution and sources of PAN and related ozone impacts is given by L. K. Whalley et al. (unpublished manuscript, 2006). Observations of $HO_2 + RO_2$ in a variety of air mass types are discussed by A. E. Parker et al. (unpublished manuscript, 2006). The impact of biomass burning emissions on the composition of the North Atlantic atmosphere is discussed by *Cook et al.* [2006]. Alkyl nitrate observations and their evolution and covariance with other trace gases is discussed by C. E. Reeves et al. (Alkyl nitrates in outflow from North America over the North Atlantic during ITOP 2004, submitted to *Journal of Geophysical Research,* 2006, hereinafter referred to as Reeves et al., submitted manuscript, 2006). Aerosol dependence on air mass types from ITOP is made by P. Williams et al. (unpublished manuscript, 2006).

3. Identifying Characteristics of Air Masses

3.1. Vertical Distribution

[11] The very nature of aircraft campaigns is such that they provide only a brief snapshot of chemical composition, without doubt undersample spatially their study domain and therefore yield data which may not, in reality, be representative of the wider Atlantic regions. Comparisons between years/data sets must therefore take account of this, and inform only in a general manner rather than on a case study basis. Despite potential undersampling it is worthwhile to compare these ITOP vertical distributions with those measured also from the Azores in flights made during April and September 1997 as part of the ACSOE programme. The details of these observations are reported by *Reeves et al.* [2002]. Figure 1a shows a comparison of the mean O_3 profiles obtained in 2004 and 1997. The mean O_3 profiles are broadly comparable between years. The most significant differences occur within the boundary layer. The mean and standard deviation in O_3 concentrations in the lowest kilometer of the atmosphere during April 1997, July 2004 and September 1997 were 36 ± 13, 24 ± 10 and 16 ± 8 ppbv respectively. These values are inline with the observed North Atlantic spring maximum–summer minimum such as those seen at Mace Head [*Monks*, 2000; *Derwent et al.*, 1998] but are roughly 6 ppbv lower than those at Mace Head because of the more southerly location of the ITOP campaign. Within the free troposphere there is little significant difference in mean profile, although the maxima occur at different altitudes levels. The locations of O_3 maxima are strongly influenced by the long-range transport of pollu-

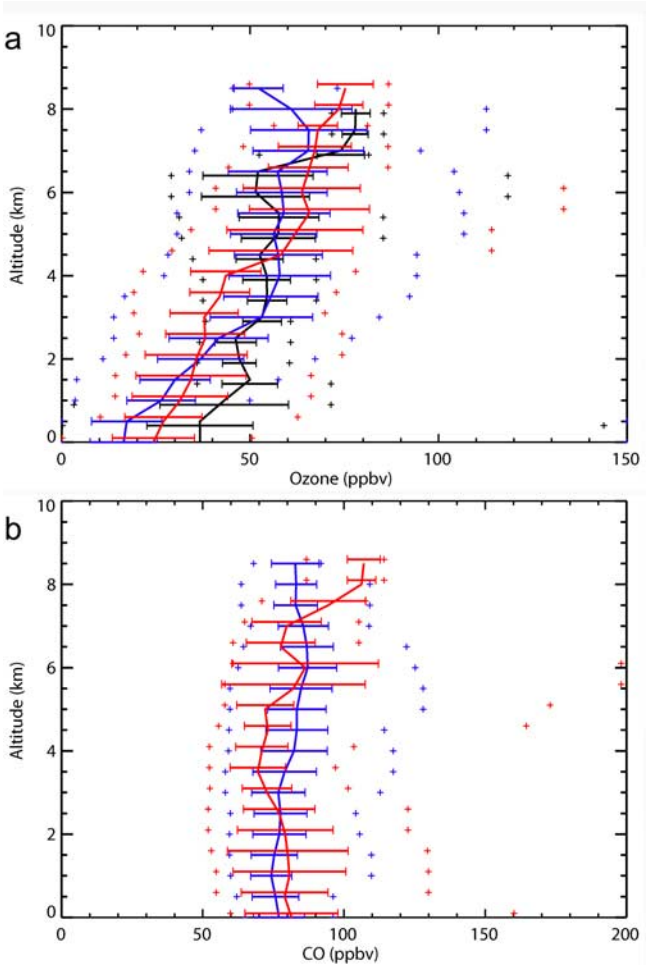

Figure 1. (a) Vertical distribution of ozone, during the ITOP campaign during July/August 2004 (red) and the ACSOE campaigns during September 1997 (blue) and April 1997 (black). Vertical lines represent the mean values half a kilometer above and below. Solid bars represent the standard deviation within the observations half a kilometer above and below. Crosses represent the maximum and minimum observed values within half a kilometer above and below. (b) Vertical distribution of CO during the ITOP campaign during July/August 2004 (red) and the ACSOE campaigns during September 1997 (blue). Vertical lines represent the mean values half a kilometer above and below. Solid bars represent the standard deviation within the observations half a kilometer above and below. Crosses represent the maximum and minimum observed values within half a kilometer above and below.

tants, the level at which each occurs being determined by individual meteorological events.

[12] A similar comparison is made between September 1997 and July 2004 CO profiles in mid North Atlantic and is shown in Figure 1b (CO observations were not available for April 1997). Compared to O_3 profiles, the difference between the two CO profiles looks less pronounced. During the 2004 campaign there is some suggestion of higher mean boundary layer CO values, lower mid tropospheric CO values, and again higher upper tropospheric CO values compared to the September 1997 values. Within the boundary layer these differences do not appear to be significantly different although variability was clearly higher in 2004. There are some very high CO values (indicated by the maximum values shown by the crosses) during the 2004 campaign in the mid troposphere associated with biomass burning plumes that were observed in this region (see sections 3.3 and 4.1). The boundary layer CO observations are roughly 10 ppbv lower than those observed at Mace Head [*Derwent et al.*, 1998] again reflecting the lower latitude of the Azores.

[13] We conclude that the CO and O_3 observations made during the ITOP campaign in July 2004 are consistent with and comparable to similar observations made in April and September 1997. Differences between the data sets can be rationalized with known annual cycles in the boundary layer concentration of O_3 and CO, and with the unusually intense North American biomass burning that occurred in 2004. The lower concentrations of O_3 and CO observed during this campaign in comparison to Mace Head are consistent with the lower latitude of the Azores. We now investigate the different air mass types observed during 2004 and attempt to systematically rationalize the factors controlling the distribution of trace gases within each type.

3.2. Observed Air Mass Types

[14] The observations made during 2004 show a degree of variability because of the "origin" of the air and hence its previous chemical and physical histories. A cluster analysis approach is used to classify these objectively, based solely upon their observed composition. Concentrations of O_3, CO, specific humidity, C_2H_6 and C_6H_6 from all of the flights averaged onto a 60 s time base, were used in an Eulerian distance minimization cluster approach [*Everitt*,

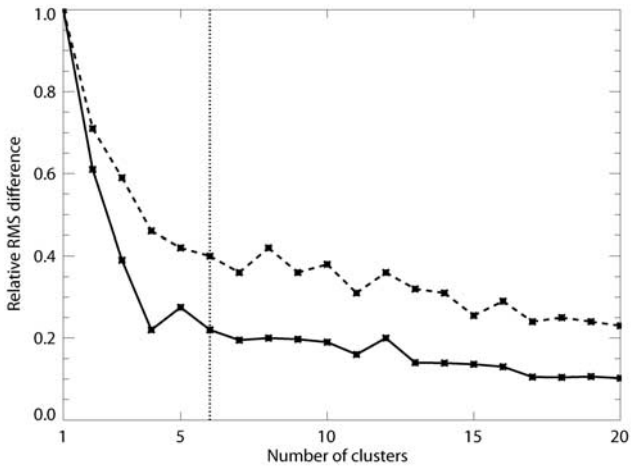

Figure 2. Sum over clusters of the RMS difference between observations within a cluster and the cluster mean, for varying number of clusters. The variables considered are logs of observed quantities, normalized to have a mean of zero and standard deviation of unity. The solid line shows the sum of the RMS results over the five variables used in the cluster analysis (derived from O_3, CO, q, C_2H_6, C_6H_6), and the dashed line shows the sum considering all variables observed by the aircraft. Both curves have been divided by the results for a single cluster and thus show the relative RMS difference.

Table 2. Mean and Standard Deviation of Selected Observations Made on the Aircraft for the Whole Campaign, Together With the Mean and Standard Deviation Within Each of the Six Clusters[a]

	All Data	Biomass	Lower Levels Outflow	Upper Levels Outflow	Moist Lower Troposphere	Marine	Upper Troposphere
% of data in cluster	100	5	26	18	36	9	6
CO, ppbV	110 ± 51	**290 ± 68**	**130 ± 20**	**95 ± 15**	**88 ± 19**	**64 ± 6.5**	**71 ± 11**
Ozone, ppbV	55 ± 19	**67 ± 4**	**61 ± 10**	**74 ± 12**	**43 ± 10**	**26 ± 10**	**78 ± 11**
H_2O, ppmV	8200 ± 6400	**410 ± 110**	**6500 ± 4000**	**2400 ± 2000**	**13000 ± 4600**	**16000 ± 5500**	**840 ± 1000**
Ethane, pptV	870 ± 430	**2300 ± 820**	**1000 ± 140**	860 ± 160	**730 ± 140**	**420 ± 89**	**650 ± 120**
Benzene, pptV	38 ± 62	**270 ± 150**	42 ± 16	**23 ± 11**	**24 ± 12**	**13 ± 11**	**9 ± 7.5**
Relative humidity, %	56 ± 28	**9 ± 4**	**52 ± 22**	**38 ± 19**	**75 ± 16**	**78 ± 15**	**16 ± 14**
Altitude, m	3700 ± 2300	**6000 ± 730**	3500 ± 1700	**6100 ± 1900**	**2400 ± 1400**	**1700 ± 1300**	**6700 ± 2300**
Pressure, hPa	680 ± 180	**500 ± 46**	690 ± 140	**500 ± 120**	**780 ± 120**	**850 ± 130**	**470 ± 160**
Latitude, deg	41 ± 3.5	41 ± 0.15	**43 ± 2.5**	**40 ± 3.5**	40 ± 4	**38 ± 2.2**	**39 ± 2.9**
Longitude, deg	−29 ± 6.6	−28 ± 2.7	−30 ± 5.4	−28 ± 9	**−28 ± 6**	**−33 ± 5.6**	**−33 ± 7.2**
Temperature, K	280 ± 13	**260 ± 6.4**	280 ± 9.3	**260 ± 12**	**280 ± 7**	**290 ± 6.5**	**260 ± 17**
Solar zenith, deg	34 ± 12	35 ± 4.3	**32 ± 8.3**	35 ± 11	**37 ± 15**	33 ± 9.3	**26 ± 6.3**
Sulfate, $\mu g/m^3$	0.36 ± 0.96	**0.04 ± 0.08**	**0.56 ± 1.6**	**0.09 ± 0.12**	0.44 ± 0.83	0.39 ± 0.41	**0.08 ± 0.13**
Ammonium, $\mu g/m^3$	0.07 ± 0.21	0.05 ± 0.11	**0.1 ± 0.26**	**−0.01 ± 0.19**	0.078 ± 0.17	**0.12 ± 0.16**	**−0.02 ± 0.20**
Organics, $\mu g/m^3$	0.39 ± 0.77	**2.1 ± 1.5**	**0.61 ± 0.94**	**0.21 ± 0.31**	**0.26 ± 0.49**	**0.14 ± 0.4**	**0.02 ± 0.26**
Nitrate, $\mu g/m^3$	0.02 ± 0.07	**0.08 ± 0.06**	0.03 ± 0.04	**0.01 ± 0.02**	0.02 ± 0.03	0.04 ± 0.2	**−0.00 ± 0.03**
CN, #/cm^3	810 ± 800	810 ± 150	**960 ± 710**	**430 ± 470**	**950 ± 960**	880 ± 850	**410 ± 310**
PAN, ppbV	0.28 ± 0.45	**1.9 ± 0.54**	**0.21 ± 0.21**	**0.35 ± 0.19**	**0.05 ± 0.06**	**0.01 ± 0.03**	**0.42 ± 0.17**
Ethane, pptV	44 ± 120	**410 ± 380**	33 ± 24	**19 ± 10**	**25 ± 17**	27 ± 18	**15 ± 14**
Propane, pptV	100 ± 100	**400 ± 190**	**120 ± 42**	110 ± 51	**64 ± 31**	**29 ± 21**	110 ± 210
Propene, pptV	10 ± 6.1	11 ± 4.2	**11 ± 5.7**	**8.9 ± 3.9**	9.8 ± 5.9	**12 ± 11**	**8.1 ± 3.3**
Iso-butane, pptV	23 ± 150	**76 ± 130**	7.9 ± 4.9	11 ± 11	6.1 ± 3.8	6.6 ± 6	**240 ± 660**
n-butane, pptV	17 ± 38	**100 ± 120**	14 ± 7.8	16 ± 22	6.6 ± 4.3	7.1 ± 4	16 ± 39
Propadiene, pptV	4.8 ± 2.3		3.8 ± 0.23		4.4 ± 0.81		
Acetylene, pptV	110 ± 140	**650 ± 260**	140 ± 51	84 ± 28	66 ± 25	34 ± 16	59 ± 18
t-2-butene, pptV	4.6 ± 1.8	4 ± 1.2	5 ± 1.7	4.3 ± 1.5	4.5 ± 1.8	4.5 ± 2.8	
1-butene, pptV	11 ± 8.2	**4.9 ± 2**	13 ± 7.4	9.6 ± 4.2	12 ± 11	11 ± 5.6	
Iso-butene, pptV	16 ± 8	**11 ± 3**	20 ± 9.4	14 ± 6.1	15 ± 7.6	14 ± 5.8	
Cis-2-butene, pptV	5.2 ± 3.6		3.4 ± 4.1				
Cyclo-pentane, pptV	9.6 ± 2	**12 ± 2**	**9.2 ± 2**	9.4 ± 2.2	9.6 ± 1.8	9.9 ± 1.9	10 ± 1.5
Iso-pentane, pptV	6.7 ± 4.4	**8.5 ± 4.5**	**5.8 ± 3.1**	7.3 ± 4	5.1 ± 3.2	6.9 ± 8.7	5 ± 3.1
n-pentane, pptV	7.6 ± 11	**27 ± 18**	**4.3 ± 2**	**4.4 ± 1.7**	**4.3 ± 2.7**	6.7 ± 7.3	6.8 ± 2.6
1−2 butadiene, pptV	3.3 ± 1.3	3.3 ± 0.35	3 ± 1.2	**2.7 ± 0.54**	**4 ± 1.9**	3.6 ± 1.3	
1−3 butadiene, pptV	16 ± 13	21 ± 14				9.4 ± 5.3	
Propyne, pptV	22 ± 6.6		22 ± 6.4	21 ± 6.2	23 ± 7.5	22 ± 5.9	21 ± 5.3
2+3 Me pent, pptV	5.3 ± 2.2	5.9 ± 2					
n-hexane, pptV	8.1 ± 8.7	**12 ± 11**	**4 ± 1.5**				
Isoprene, pptV	2.8 ± 0.81						
dms, pptV	30 ± 26	35 ± 16			22 ± 9.9	39 ± 35	
Octane, pptV	12 ± 9	9.3 ± 5	14 ± 11				
Toluene, pptV	10 ± 18	**43 ± 41**	11 ± 14	**3.6 ± 1.1**	**5.6 ± 2.7**	5.9 ± 2.4	4.7 ± 1.7
Acetaldehyde, pptV	1700 ± 1500	**1000 ± 410**	**2400 ± 1900**	**1200 ± 400**	1500 ± 750	**2100 ± 2900**	**1200 ± 800**
Methanol, pptV	830 ± 610	**2500 ± 1100**	**1100 ± 570**	**680 ± 260**	**630 ± 220**	**530 ± 320**	**380 ± 260**
Acetone, pptV	1200 ± 490	**1900 ± 300**	**1500 ± 580**	1200 ± 250	**990 ± 240**	**760 ± 250**	**680 ± 230**
HCHO, pptV	470 ± 520	440 ± 240	400 ± 570	**180 ± 260**	620 ± 580	**590 ± 450**	520 ± 340
Inorganic peroxide, ppbV	0.46 ± 0.64		**0.26 ± 0.55**	0.5 ± 0.63	**0.68 ± 0.73**	0.43 ± 0.51	**0.24 ± 0.4**
Organic peroxide, ppbV	0.28 ± 0.34		**0.12 ± 0.26**	0.24 ± 0.31	**0.42 ± 0.34**	0.48 ± 0.41	0.26 ± 0.28
ΔP over last 5 days, hPa	−18 ± 155	46 ± 148	−10 ± 167	−106 ± 169	−35 ± 142	14 ± 112	60 ± 114
Δ theta over last 5 days, hPa	−0.6 ± 15.2	8.8 ± 19.1	−1.4 ± 14.5	−9.8 ± 17.3	−2.6 ± 10.0	0.1 ± 7.9	8.5 ± 14.3

[a]Those elements in the table which are in bold show observations within a cluster which have significantly different mean values from those observations not in the cluster (i.e., cluster 1 versus the mean of clusters 2 to 6) at the 95% confidence limit using a student-t test.

1993]. These five variables were selected because they have good coverage across the data set and are expected to distinguish polluted air masses (higher CO, C_2H_6 and C_6H_6) from clean ones, upper tropospheric air masses (lower specific humidity, higher O_3) from lower tropospheric ones, and biomass burning from anthropogenic plumes (the relative proportions of CO, C_2H_6 and C_6H_6). Simultaneous observations of all five parameters were available for a total of 843 60 s intervals. Differences in their variability were removed by taking logarithms and normalizing to give all transformed variables a mean of zero and a standard deviation of unity. This cluster approach attempts to classify the sets of observations of the five chosen variables over the entire campaign into a given number of clusters such that the distance (in transformed variable space) between the individual observations within each cluster are minimized.

[15] The number of clusters to calculate is not known a priori. In order to find an optimum number of clusters, the clustering was performed with between 1 and 20 clusters. The success of the clustering was evaluated by calculating the root mean square (RMS) difference between each observation and the mean value of observations within its cluster (Figure 2). This was calculated for just those species included in the cluster analysis (CO, O_3, H_2O, C_2H_6, and

C_6H_6) and for all the species measured on the aircraft. Values have been normalized to give a root mean square difference of unity for the case with one cluster. A rapid reduction in the RMS difference occurs between one and six clusters, with a slower reduction beyond this point. Six clusters were chosen as representative of the dominant air mass types, a balance between having many clusters based around individual events or a few clusters with indistinct composition.

[16] Table 2 shows the mean and standard deviation value of those species observed on the aircraft for the whole campaign (all flights), together with the mean and standard deviation value of those species within each of the six clusters. The emboldened elements in Table 2 highlight species within a cluster that are significantly different from those not in the cluster (i.e., cluster 1 mean versus the mean of clusters 2 to 6) at the 95% confidence limit using a student t-test.

[17] Figure 3 shows the probability distribution functions (PDFs) for those species used in the clustering (CO, O_3 specific humidity, C_2H_6, and C_6H_6) and PAN for each of the cluster types and for the complete data set. There is a good degree of separation for some species within some clusters showing distinct compositional signatures. For example the O_3 and H_2O distributions within the ''marine'' cluster are on simple visual inspection very different to those in the ''upper troposphere.'' The CO, PAN and hydrocarbons within the ''biomass burning'' cluster are significantly higher than within the other clusters.

[18] Figure 4 shows the relationships between the key species and CO within each cluster. The biomass burning cluster contains the highest concentrations of CO and the hydrocarbons, with lower concentrations in the polluted outflow clusters and in the moist mid troposphere. The marine boundary layer and the upper troposphere show the lowest concentrations of CO and hydrocarbons. The observed relationship between O_3 with CO is highly dependent on both location and the history of an air mass, however mixing of differing air masses can result in a relationship which is complex to disentangle, as seen in previous campaigns [see, e.g., *Parrish et al.*, 1998]. Within the marine boundary layer there is low CO and this is associated with low O_3. This contrasts to the upper troposphere where low CO is associated with high O_3. The very high CO associated with the biomass burning does not seem to lead to rapid O_3 production (see section 4.1). This cluster is distinguished by a much higher ratio of benzene to ethane.

[19] These six clusters are classified according to the PDFs of composition and correlations between species, as follows. The first cluster (containing 5% of data set) contains very high concentrations of CO, hydrocarbons, PAN, and aerosol phase organics. We attribute this to interceptions of biomass burning originating from northern North America and call this ''biomass burning'' air (see section 4.1). The next two clusters we attribute to anthropogenic pollution originating from North America intercepted in the lower (26% of data set) and mid/upper troposphere (18% of data set) respectively (''Lower Level Outflow'' and ''Upper Level Outflow''). They contain moderately high concentrations of CO, some longer-lived hydrocarbons, and small oxygenate such as acetone and methanol. The lower level outflow is most readily distinguished from the upper level outflow by its higher water vapor content, high aerosol loadings and lower PAN (see sections 4.2 and 4.3). The fourth cluster is attributed to moist lower to mid tropospheric air and contains the most observations of any cluster, with 36% of the data set (''Moist Lower Troposphere''). This can be considered the general background air observed during the campaign. The fifth cluster (9% of data set) represents a highly processed marine boundary layer with low concentrations of primary pollutants such as CO, hydrocarbons and low concentration of species such ozone and PAN (''Marine''). It also contains high concentrations of DMS which is released in these regions from the ocean surface. The sixth cluster (5% of data set) is very dry and has high ozone, low carbon monoxide and higher PAN and is attributed to the relatively clean cold upper troposphere air (''Upper Trop'').

[20] The consistency of these cluster attributions is analyzed through the use of the back trajectories. Back trajectories were calculated for points every 10 s along the flight tracks using the ECMWF analyzed winds at 1.125° resolution using the code of *Methven* [1997]. Figure 5 shows the locations of air masses over the 5-day interval before being sampled by the aircraft, partitioned by cluster. There is a surprising degree of consistency between the attribution made from the chemical composition and those from the meteorological analysis. The biomass burning cluster trajectories all show transport from northern Canada/Alaska consistent with the biomass burning events discussed in *Pfister et al.* [2005]. The two polluted outflow clusters show trajectories that in general spend some time over the continental US and then are transported to the Atlantic region. The marine trajectories show little contact with continental regions and spend most of their time confined to the lower troposphere. If these trajectories are traced back even further than 5 days many of them spend extended periods (up to the 10 days length of the longest trajectories) caught up in the Azores/Bermuda high system well away from anthropogenic pollution. The upper tropospheric trajectories show origins within the mid to upper troposphere.

[21] Further sections of this paper will aim to identify the chemical characteristics of air masses as encountered on certain individual flights, and make links to the cluster type into which this case study may fall. The primary objective of the ITOP project was to investigate the transportation of polluted air masses as they cross the North Atlantic from the North America to Europe. Thus specific attention is given the biomass burning and the outflow events that were observed.

4. Case Studies Highlighting the Different Air Mass Types

4.1. Biomass Burning Air Masses

[22] The cluster analysis attributes the most significant elevations in both CO and many other tracers to a single cluster that was intercepted predominantly between 4500 and 6500 m. These air masses can be clearly tied to boreal forest fire plumes originating in northern Canada and Alaska. These are featured in detail in a number of ICARTT papers including *Pfister et al.* [2005], *Cook et al.* [2006], and *Real et al.* [2006]. These papers focus on aspects such

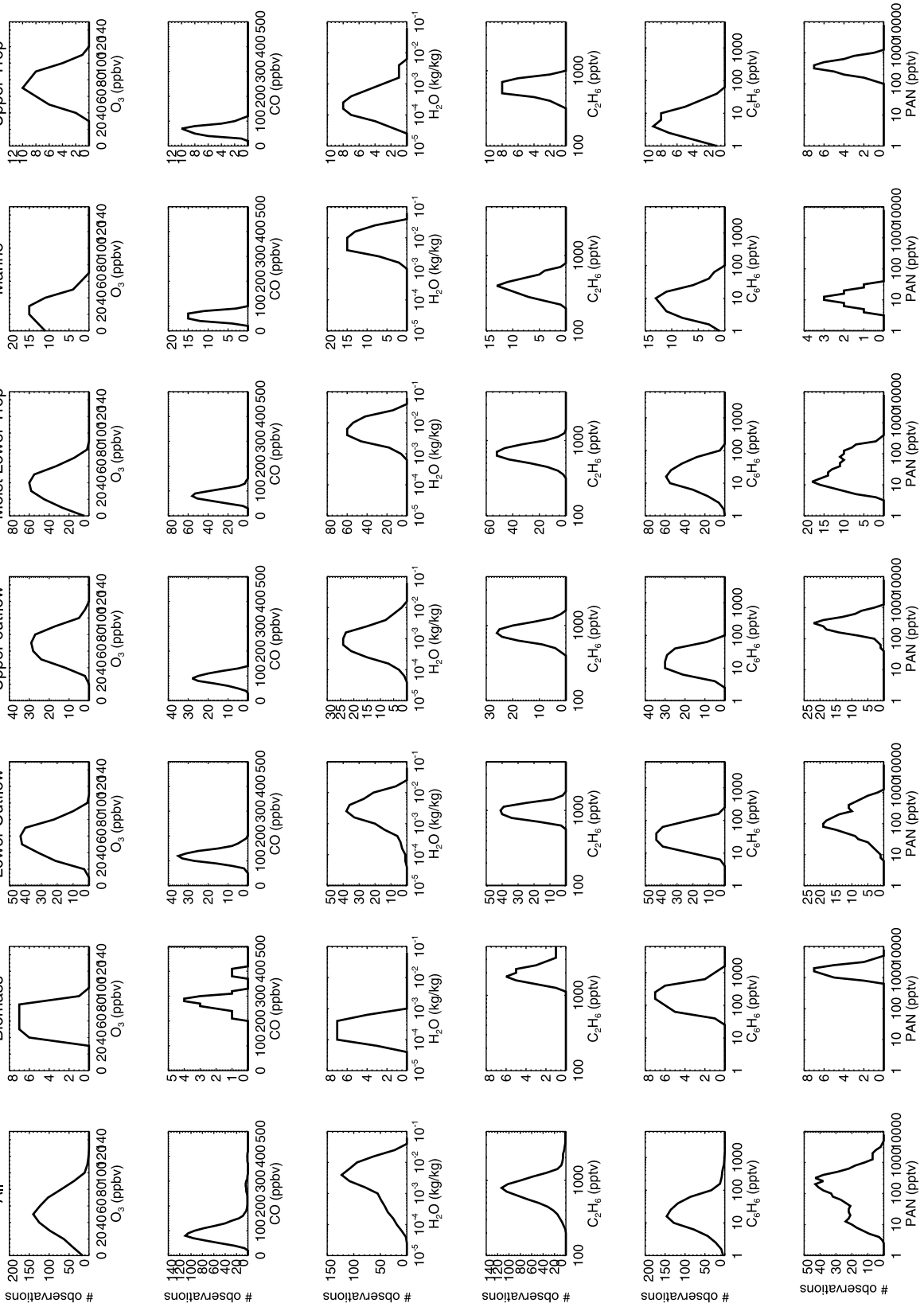

Figure 3. Histograms of the concentrations in each of the six clusters identified objectively and the full data set.

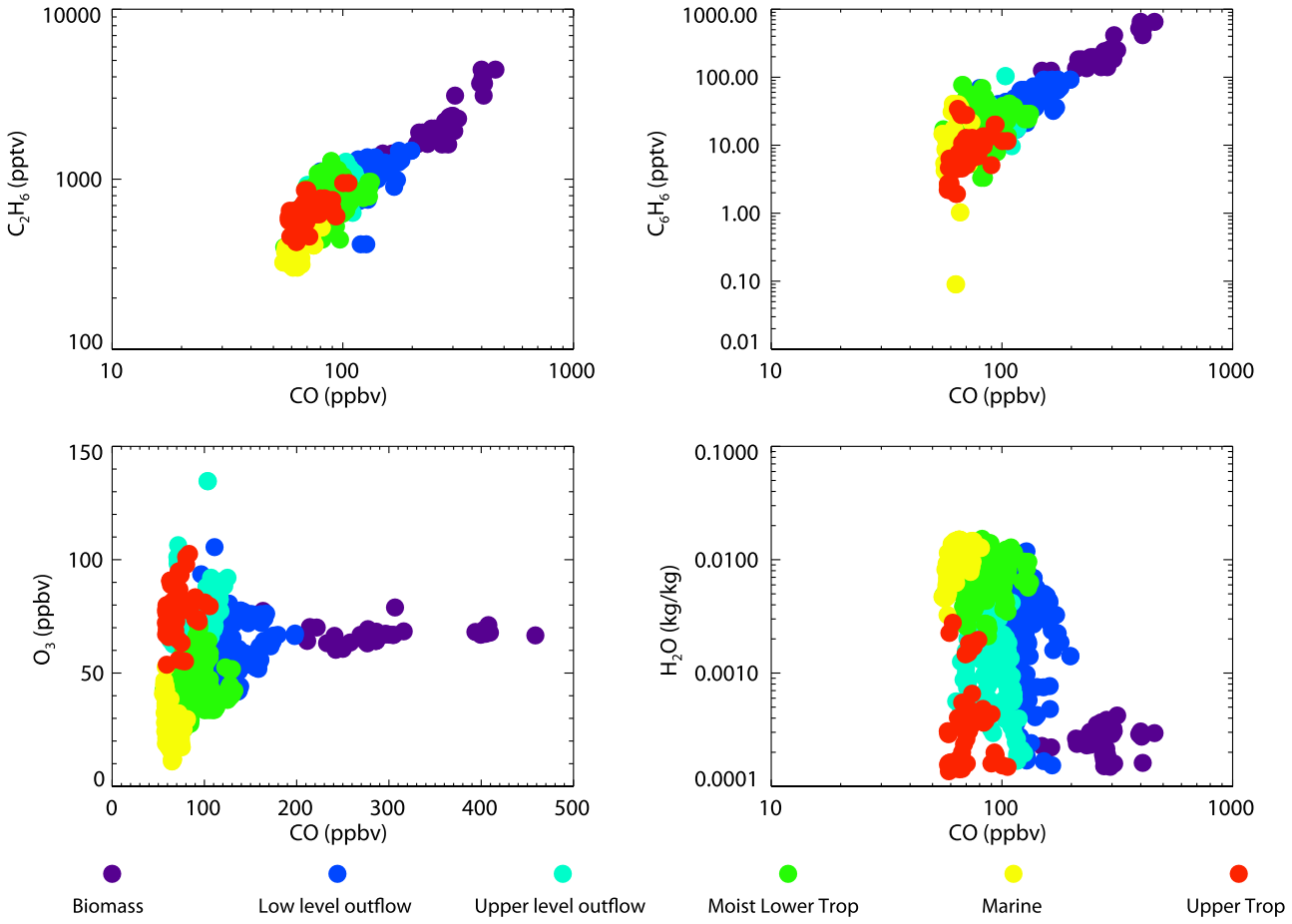

Figure 4. Relationship between key species and CO within each cluster. Colors represent biomass (purple), low level outflow (dark blue), upper level outflow (light blue), moist lower troposphere (green), marine (yellow) and upper tropospheric (red) points.

as pollutant injection height, the fire extent and the transport and evolution of CO and O_3 assessed by both aircraft and satellite observations. Distinct and identifiable interceptions with biomass burning plumes occurred on seven ITOP flights (marked as B on Table 1). Often weaker influence of biomass plumes was encountered on mixing with surrounding air masses notably on 31 July and 1 August flights. The biomass burning plumes encountered in ITOP were often thin in the vertical. As a result there was sometimes only limited sampling within each plume, notably for whole air samples, and our knowledge on plume extent was obtained from fast responding instruments such as CO, NO and organics via PTR-MS. The biomass burning air masses encountered in mid Atlantic contained a very distinct distribution of chemical markers; CO, ethene, acetylene, benzene and PAN being substantially elevated compared to other air mass types.

[23] The 29 July flight (B036) encountered a biomass burning air mass in addition to pollutants of anthropogenic origin uplifted via a warm conveyor belt (discussed further in section 3.7). The time series of data in Figure 6 is annotated for these two major air mass types and shows a clear plume region encountered early in the flight with ozone, ethene, PAN and CO elevation. When considered within the context of the whole flight, CO and O_3 show simultaneous increases in concentration during this plume interception perhaps suggesting a photochemical production of O_3 within the biomass burning plumes. When considered in isolation, however, the CO and O_3 within the biomass burning plume anticorrelate (Figure 7), complicating the picture.

[24] Although interceptions of different biomass burning plumes occurred over a range of different flights and locations, the overall chemical signatures of biomass burning plumes are similar. This was notably the case for elevated primary emissions markers such as CO, ethene and benzene. However, there is not a single canonical relationship between CO and O_3 within all biomass burning plumes. The 20 July observations (flight B032) provide a further example of a major plume interception, although in a slightly colder air mass than that of the 29 July example (20 July plume average 263 K versus 29 July, 268 K) at a similar altitude of 6000 m. In the cooler air mass PAN was found in much higher concentrations, up to 4000 pptV, and with CO up to 600 ppbV. Figure 8 shows the time series data for the interception of biomass burning plumes during this "colder" flight. In this case it is clear that there is no elevation in O_3 within the plume itself when compared to

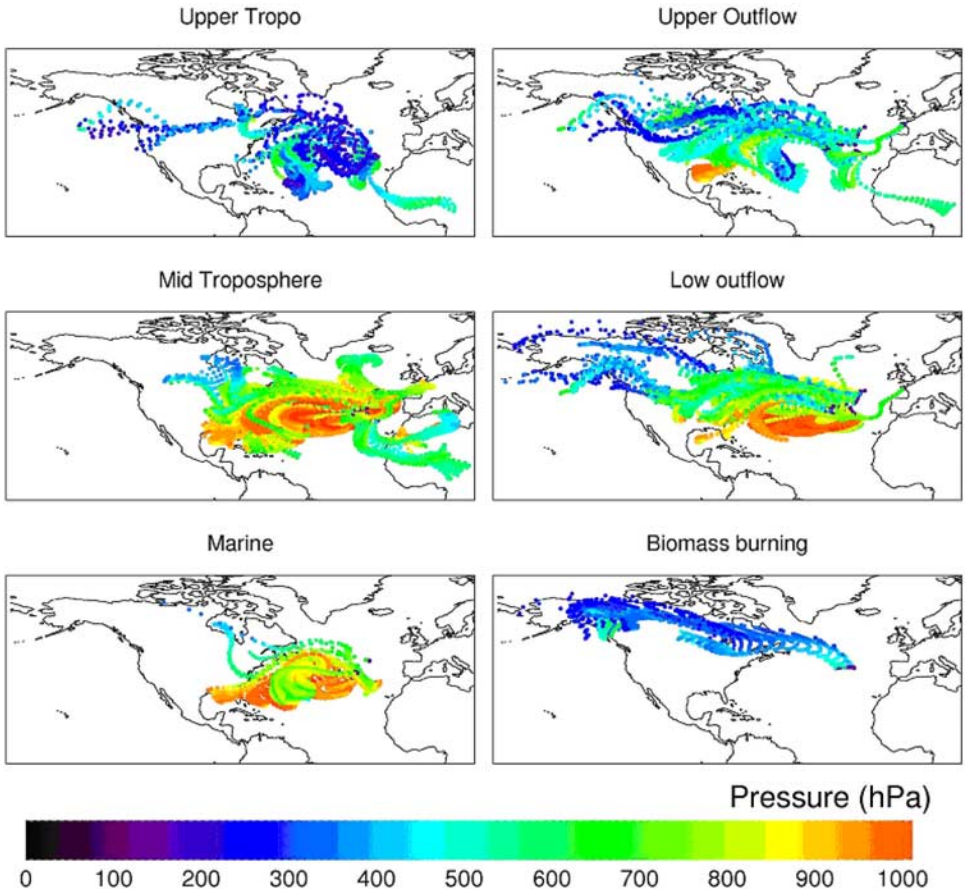

Figure 5. Five-day back trajectories from sample points on all ITOP-UK flights partitioned using the cluster label assigned to each sample on the basis of its composition. Colored circles represent position every 6 hours along trajectories. Pressure is indicated by the color of the circle.

surrounding background free troposphere regions. A comparison of CO/O_3 relationships inside and outside of the biomass plume for this flight is shown in Figure 9. Again this shows an anticorrelation between O_3 and CO within the plume.

[25] The biomass burning plume on 20 July was also intercepted near Newfoundland on 18 July by the NASA DC8 and above France on 23 July by the DLR Falcon. *Methven et al.* [2006] refer to this multiple interception as ''Lagrangian case 2'' and the matching trajectories are shown in that paper. Ozone is observed to increase between the DC8 and BAe146 by 5.9 ± 2.9 ppbv and then by 11.4 ± 3.8 ppbv en route to the Falcon. This is discussed in detail by *Real et al.* [2006] where they have initialized photochemical models with the composition observed by the NASA DC8 and shown that ozone is photochemically produced following the trajectory toward the FAAM BAe146 and then DLR Falcon by an amount consistent with the change inferred from the observations. They subsequently explore the sensitivity of ozone production to the reduction of photolysis rates associated with absorption and scattering by the aerosol in the plume itself. They also show that the slope of the CO/O_3 scatterplot is most negative in the plume observed by the NASA DC8 and that the increase in slope with time can be explained by photochemical production of ozone. The negative slope may have been established near the forest fires, although the NASA DC8 is estimated to have been 3 days downwind of the source. A plausible argument is that ascent in pyroconvection is so fast that NO_x is rapidly converted to PAN before much ozone production occurs, or the plume may even be in a net ozone loss regime. Then mixing between the high CO, low ozone air detraining from the pyroconvective plumes and the low CO, high ozone of the surrounding air in the upper troposphere would result in a negative slope.

[26] A remarkable feature within this colder encounter was the elevation of ethene seen at 1500 pptV in the centre of the plume (compared with ~120 pptV from B036). This value is however consistent with the even higher concentration measured upwind by the NASA DC8 and loss by reaction with OH [*Methven et al.*, 2006]. Arnold et al. (submitted manuscript, 2006) have further shown that the links between these flights are sufficiently good that it is possible to quantify the average [OH] and dilution rate experienced between the DC8 and Falcon.

[27] Biomass burning air masses were encountered not only from aircraft within the ICARTT consortium, but also seen frequently throughout the entire summer 2004 by the

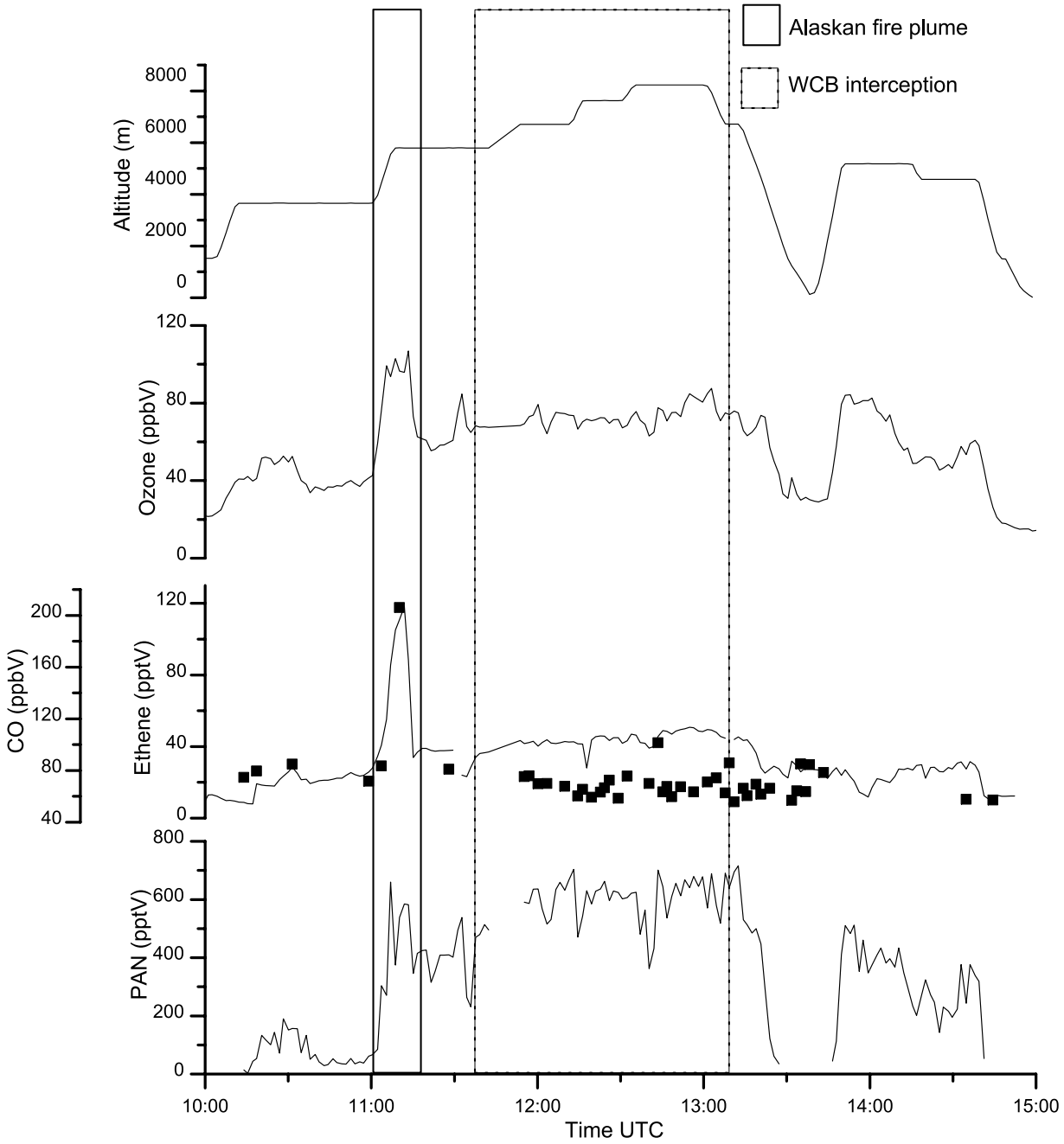

Figure 6. Time series of data from flight B036 on 29 July 2004, averaged over 90 s windows. Altitude (m), O_3 (ppbv), CO (ppbv), ethene (black squares) (pptv) and PAN (pptv) are shown. Alaskan fire plume and warm conveyor belt (WCB) interceptions are highlighted.

Pico observatory and are reported by *Val Martín et al.* [2006].

4.2. Low Level Continental Outflow Into the Mid-Atlantic Region

[28] Flights undertaken on nine occasions were distinctive in that boundary layer pollutants from the US central and east coast regions were transported toward the Azores at relatively low level (>500 hPa). These flights are marked on Table 1 designated "L." The cluster analysis identifies this as the "Lower Level Outflow" cluster. These air masses are characterized by elevated concentrations of CO, aerosol components, hydrocarbons and oxygenates, moderate temperatures, relative humidity, and PAN.

[29] Such an air mass was encountered by flight B031 on 19 July 2004. This example is especially interesting because it was intercepted upwind on 15 July by the NASA DC8 and NOAA WP3-D and downwind on the 22 July by the DLR Falcon and again on the 25 July by the FAAM BAe146. Together these interceptions are labeled "ICARTT Lagrangian case 1" by *Methven et al.* [2006].

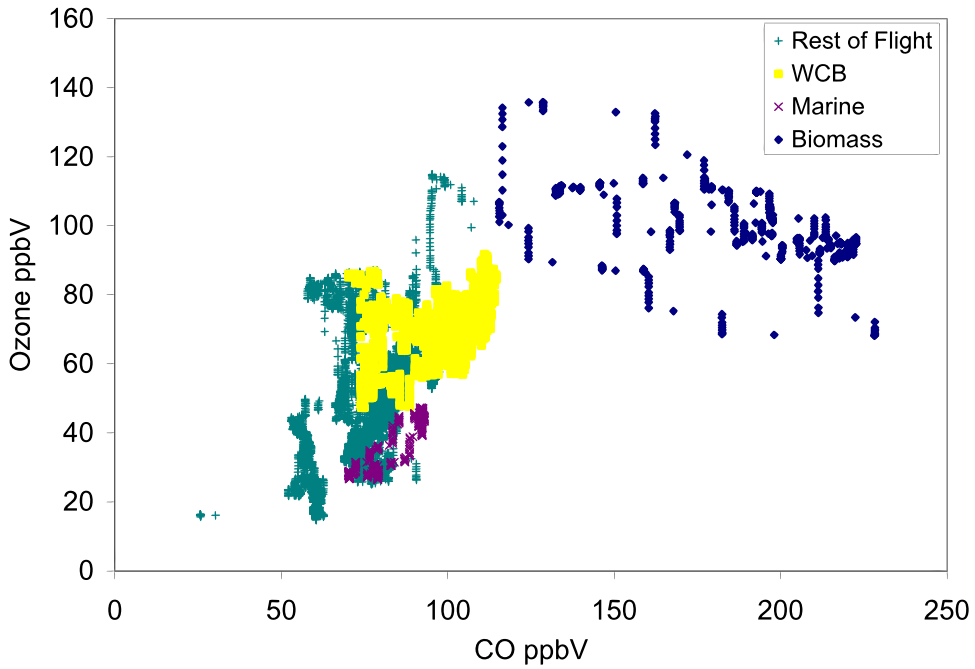

Figure 7. CO/O_3 relationships for flight B036 on 29 July 2004, colored by air mass type.

[30] Figure 10a shows the calculated mixing ratio of an anthropogenic emissions tracer in the region of the Azores on the 950 hPa surface for the 19 July. Four day back trajectories were calculated from the ECWMF analyzed winds, from a grid filling the shown domain with 0.75° × 0.50° latitude-longitude spacing and on 32 different pressure levels. If the trajectories passed over a region with anthropogenic emissions (as defined by the EDGAR NO_x emission inventory [*Olivier et al.*, 1994]) and were within the boundary layer (as identified by the ECMWF model) the emissions were accumulated along that trajectory. The initial value of the anthropogenic emission tracer was zero. We use a NOx rather than CO emissions tracer in these simulations in order to better distinguish between anthropogenic and biogenic emission sources. The final value of this tracer is shown in Figure 10a. We describe this technique as Reverse Domain Filling for a 3D domain (RDF3D) and more details of this approach are given by *Methven et al.* [2006]. It was used extensively during the campaign to plan the flight tracks of the aircraft. The track of the aircraft position in Figure 10b has been shifted using short back and forward trajectories to the single time frame used to display the emissions tracer, 12UT 19 July, so that the aircraft position relative to air masses can be better described. Figure 10b colors the flight track with observed CO concentration, showing that the pollution occurred in the location simulated by the RDF3D technique. The back trajectories were last in contact with the continental boundary layer around the New York conurbation. The RDF3D simulation using analyzed winds indicated that the highest concentrations in the pollution plume may have lain just beyond the range of the aircraft. We have not in this study attempted to calculate general forecast statistics however tracer structure and location was sufficiently well forecast (especially using latest 24 hour forecasts) that target air masses could be reliably intercepted. Routes were adjusted during flight by interpreting the real time data using the forecasts. Therefore, even though the tracer forecasts could have displacement errors, these could be compensated for during flight.

[31] A similar low level outflow event was sampled on 20 July. Both events were characterized by the highest sulfate aerosol loading (P. Williams et al., unpublished manuscript, 2006) and the highest alkyl nitrate concentrations (Reeves et al., submitted manuscript, 2006) observed during the campaign. The origin of the aerosol can be traced back to the Ohio River Valley and the coal burning power plants there.

[32] In low level outflow events, such as observed in Lagrangian case 1 on 19 July, the pollution was observed to be advected within the marine boundary layer as well as the clear air above. ICARTT observations upwind close to the east coast USA show that the high pollution levels within the continental boundary layer are advected out over the ocean. The sea surface temperature off the east coast, near Cape Cod and the Gulf of Maine, is cold and the boundary layer turbulence evolves rapidly following the flow, collapsing to a very shallow marine boundary layer. Such processes have been observed previously in the ACE-2 Lagrangian experiments [*Johnson et al.*, 2000] following polluted air masses from Europe toward the Canary Islands over the East Atlantic. The outflow within the marine boundary layer experiences ozone loss associated with deposition and photochemical loss associated with the high humidity there. The outflow in the polluted layer that remains above the marine BL is drier, often cloud free and retains higher concentrations of pollutants, especially sulfate aerosol.

4.3. Upper Level Outflow

[33] Elevation in species such as CO, NO and NMHCs were seen in the mid to upper troposphere on seven ITOP

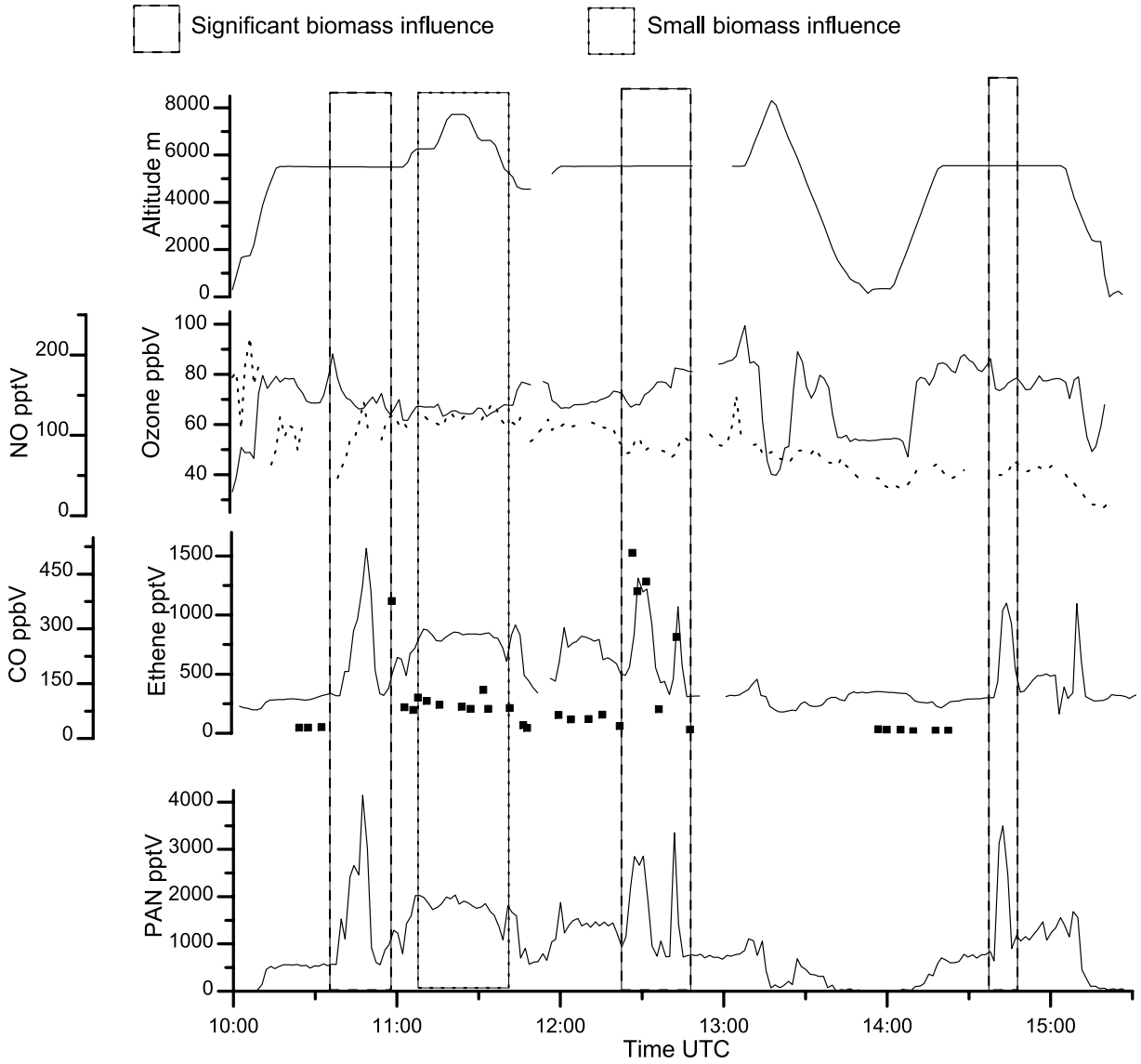

Figure 8. Time series of data from flight B032 on 20 July 2004, averaged over 90 s windows. Altitude (m), O_3 (ppbV), NO (dashed lines) (pptV), CO (pptV), ethene (black squares) (pptv) and PAN (pptV). Interceptions of biomass burning plumes are indicated. The three highest CO events highlighted in a dashed box are interceptions through the same filament structure [see *Methven et al.*, 2006].

flights with two major chemical signatures. The first, biomass burning profile has been discussed in section 4.1, while the second signature may be assigned to surface anthropogenic sources, and this is independently isolated via the cluster analysis. Two flights, on 28 and 29 July 2004, resulted in clear encounters with polluted continental boundary layer air lifted to above 500 hPa, and these interceptions fall into the cluster described as "upper level outflow."

[34] Figure 11a shows the results of a RDF3D simulation from the Azores domain at the highest pressure level reached by the BAe146 (350 hPa). The colors indicate the change in pressure experienced along trajectories between 1200 UT, 25 July and arrival on the grid at 1200 UT, 29 July. The BAe146 flight track is shown shifted relative to air masses at this instant (the trajectory arrival time). Figure 11b shows a vertical cross section through the 3D domain along the dashed line X to Y in Figure11a (using same color scale). The flight track is projected normally onto the section (method detailed by *Methven et al.* [2003]). The blue shading indicates air masses that have ascended by more than 500 hPa in 4 days. The cross section shows that these ascending trajectories form a coherent air mass in the upper troposphere and that the flight intersected it on its top runs (although not in the region that had experienced strongest ascent). Such coherent ensembles of trajectories define warm conveyor belts [*Wernli and Davies*, 1997]. The back trajectories from the vicinity of these runs match forward trajectories from the flights of the NASA DC8 on 28 and 25 July respectively [see *Methven et al.*, 2006]. We assign therefore this particular interception as occurring in a warm conveyor belt that ran along the east coast USA,

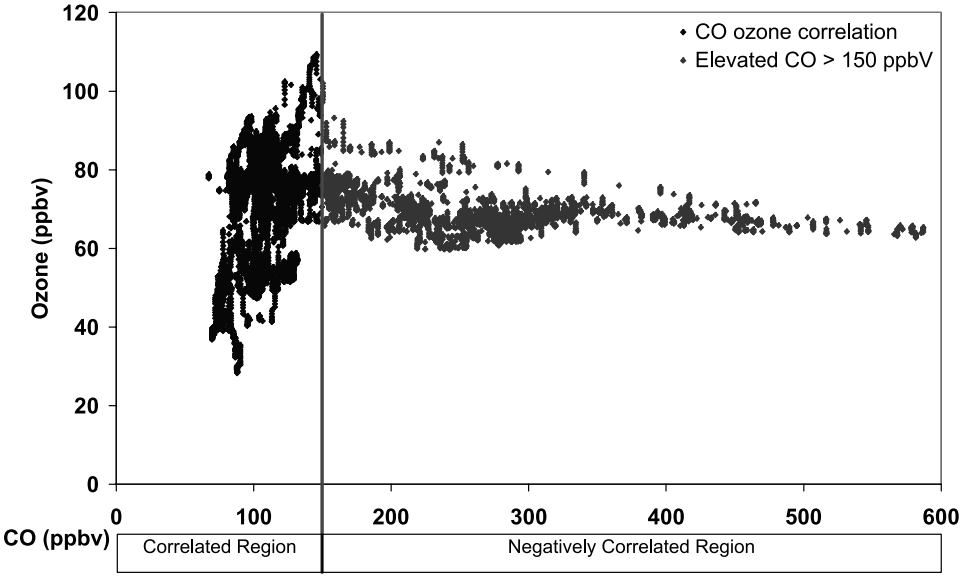

Figure 9. CO/O_3 scatterplot for flight B032 on 20 July 2004, showing the negative correlation in the Alaskan fire plume.

ahead of a cold front. There is further detail of this case study from the perspective of ozone enhancement over the USA in the work by *Cooper et al.* [2006]. *Methven et al.* [2006] have established Lagrangian links with the air sampled by the FAAM BAe146 on 29 July and the NASA DC8 on 25 and 28 July, the NOAA WP3-D on 27 July and the DLR Falcon flying over Belgium on 31 July. Together these interceptions constitute "ICARTT Lagrangian case 4."

[35] The air mass forms a complex 3D structure and so the cross section is not representative of the air encountered by the aircraft across the complete domain. Similarly, the horizontal plan only depicts air encountered by the aircraft on its highest flight legs. Nevertheless the cross section was chosen to illustrate the correspondence with observed CO. The flight projected onto a latitude-pressure section is colored by CO concentration in Figure 11d. CO is clearly elevated within the WCB. The region of highest CO is associated with the biomass burning plume (labeled on Figure 6) discussed in section 4.1. Comparing the RDF3D cross section shows that this plume had experienced descent over the last 4 days and was therefore very dry. It also

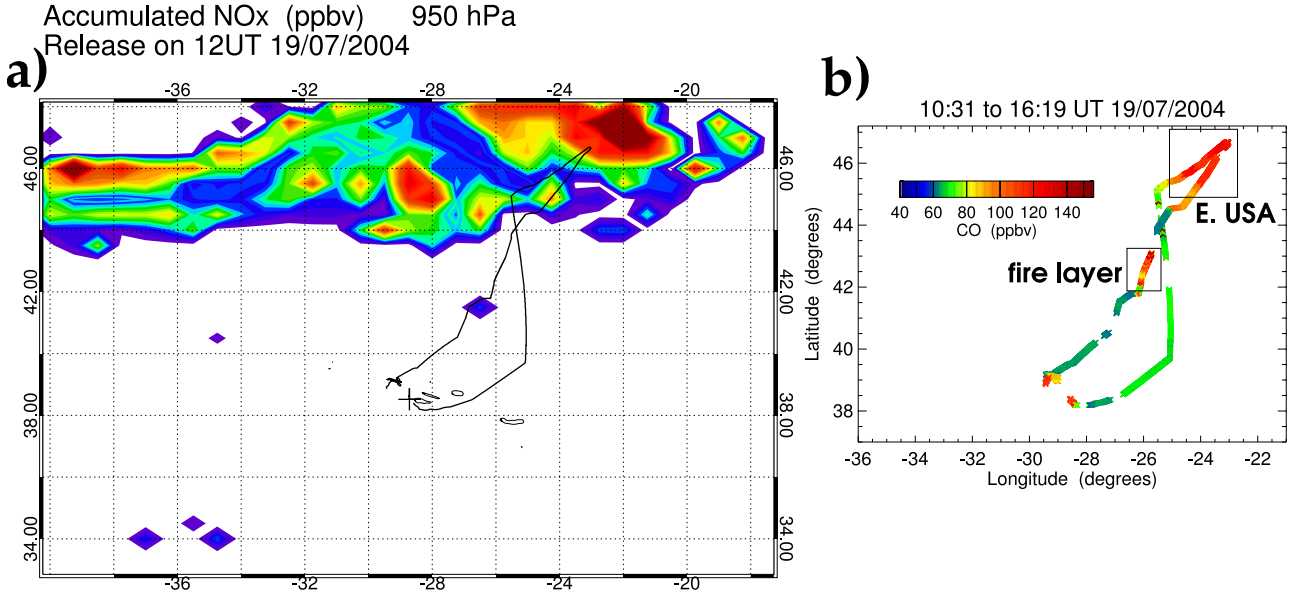

Figure 10. (a) RDF3D simulation of an anthropogenic emissions tracer (accumulated NOx) on the 950 hPa pressure level for Azores domain at 1200 UT, 19 July 2004. Color shows tracer increasing from blue to red with contour interval of 2 ppbv. Flight track B031 is shown shifted relative to the sampled air mass locations at 1200 UT. (b) Flight track colored by observed CO.

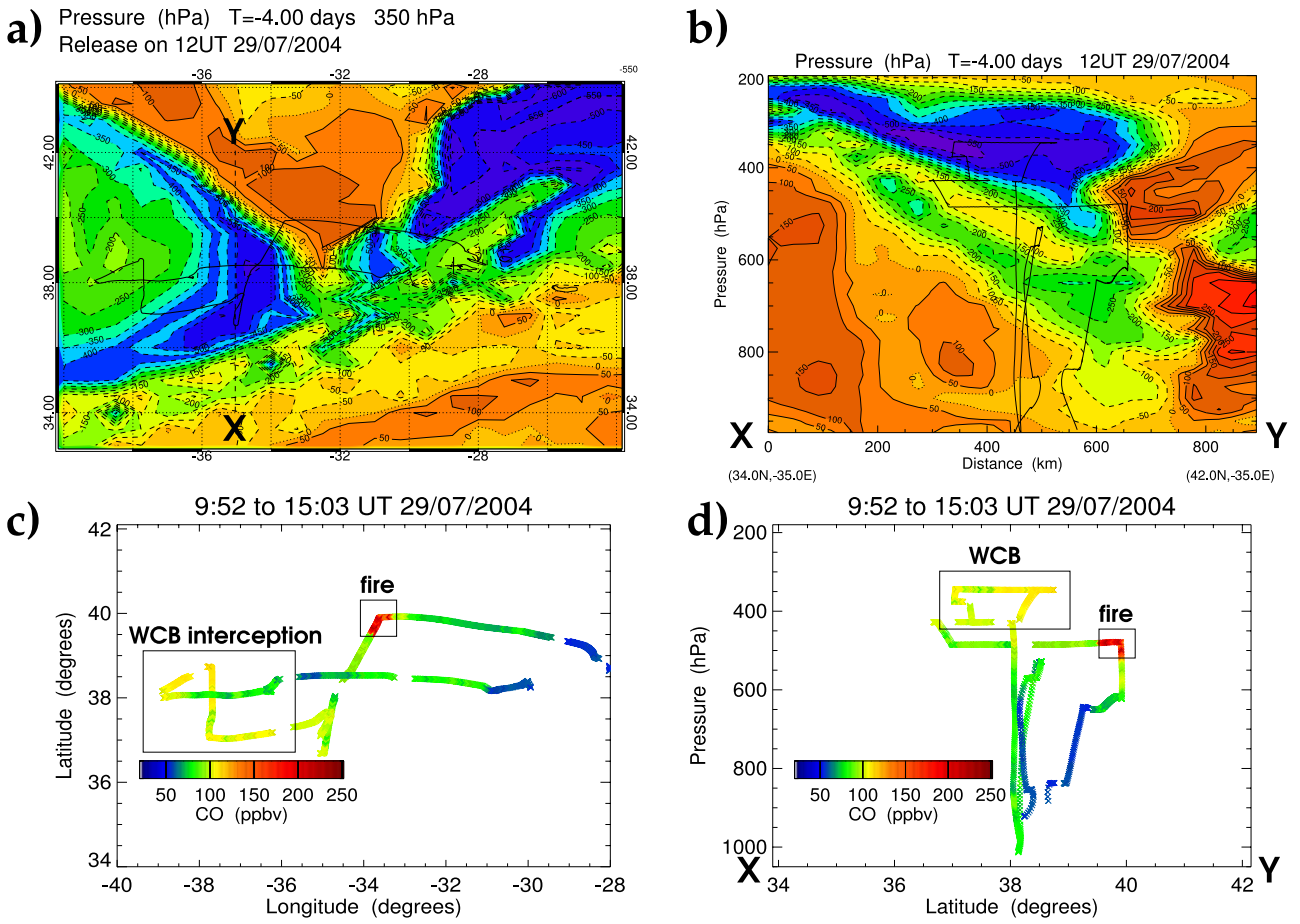

Figure 11. (a) RDF3D simulation showing change in pressure following air masses over 4 days before arrival on the 350 hPa pressure level at 1200 UT, 29 July 2004 (contour interval is 50 hPa). Air mass relative B036 flight track is overlain. (b) Cross section along 35W (dashed line XY) showing change in pressure with the same color scale. Flight track projected normally onto the section. (c) Observed CO along air mass relative flight track B036. (d) Observed CO along flight track B036 projected onto a latitude-pressure section.

originates from northern Canada and has low equivalent potential temperature because of its high-latitude origin.

4.4. Moist Lower Troposphere

[36] As frontal systems pass over the USA polluted air is advected rapidly over the ocean. Often trajectories run parallel to the east coast in a northeastward direction because the fronts are associated with weather systems that develop rapidly on the temperature contrast between the continent and ocean and the gradients in SST associated with the Gulf Stream. During the ICARTT period such a frontal passage occurred over the USA on 25–27 July. Trajectories within the middle of the warm sector originated far to the south and experienced strongest ascent, forming the warm conveyor belt sampled near the Azores on 29 July (discussed in section 4.3). Trajectories on the eastern flank of the WCB missed landfall altogether and therefore remained free of pollution. This air mass was sampled to the west of the Azores by the FAAM BAe146 and NASA DC8 during their intercomparison on 28 July.

[37] However, trajectories on the western flank of the WCB bordering the cold air mass were advected rapidly northeastward but experienced much weaker ascent, outflowing in the lower to midtroposphere behind the WCB. This air was sampled by the NOAA WP3-D on 27 and 28 July and again by the FAAM BAe146 on 31 July and 1 August. Together these interceptions constitute "Lagrangian case 5" as depicted by *Methven et al.* [2006]. This air experienced weak ascent and was therefore saturated, at least close to the USA. This event falls into the "moist lower troposphere" cluster which exhibits high sulfate aerosol concentrations, albeit lower than in the dry low level outflow. The more vigorous mixing within the frontal zone also resulted in more rapid dilution of the pollution so that its signature over the mid-Atlantic was weak. In this case, within the frontal system the low level anthropogenic outflow was overlain by air that had descended from northern Canada heading eastward across the Atlantic. This descending air was contaminated with pollution from boreal forest fires and was also sampled upwind by the WP3-D on 28 July. The frontal structure consisting of sloping layers of contrasting composition is depicted by *Methven et al.* [2006]. There is clear evidence of mixing across the front between the moist anthropogenic and dry biomass burning

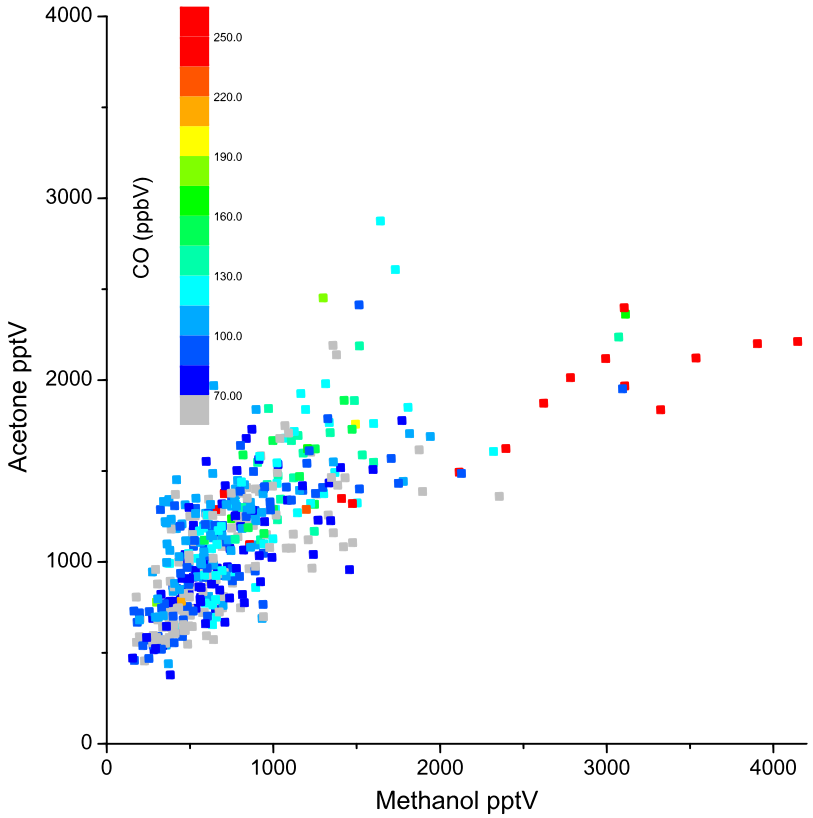

Figure 12. Methanol versus acetone scatterplot for all data from ITOP flights, colored (70 to >250 ppbV) as a function of WAS sample averaged [CO]. Grey squares indicate no coincident CO data. All methanol observations above 2000 pptV are associated with biomass burning air mass type.

layers, and the "moist lower tropospheric cluster" contains a mixture of both of these signatures.

5. VOC and OVOC Signatures

[38] Nonmethane hydrocarbons and oxygenated compounds have also been used throughout ITOP as component tracers of air mass origin. These have shown particularly high variability for such remote locations, in some instances a single species (ethene) varying over four orders of magnitude in concentration. The distribution of nonmethane hydrocarbons observed from anthropogenic North American sources was in generally good agreement with that predicted by upwind observations, decayed for subsequent reaction with OH. This is discussed further as a Lagrangian marker by *Methven et al.* [2006] and more specifically in terms of OH loss rates by Arnold et al. (submitted manuscript, 2006). Most noticeable individual features in NMHC abundance were the maxima encountered in the biomass burning plumes with particularly significant elevation in ethene (max 1500 pptV), acetylene (max 1287 pptV) and benzene (650 pptV), and a strong internal correlation between them ($R^2 \sim 0.8$).

[39] Certain oxygenated volatile organic compounds (OVOCs) were also measured and used as source tracers using samples collected in canisters with analysis by dual channel gas chromatography. Data acquired from such a sampling methods should be treated with a degree of caution because of potential problems with storage at low concentration. Measurement of acetaldehyde in the atmosphere has been specifically highlighted in the literature as problematic because of the rapid reaction with ozone within the sampling lines, an interference that may be augmented by storage in canisters prior to sampling. Samples collected during the ITOP campaign were analyzed within 48 hours of collection. Trends and ratios between OVOCs and NMHCs during ITOP observations were however closely matched to those observed during the NAMBLEX [*Lewis et al.*, 2005] campaign in 2002, where in situ measurements were made (eliminating storage problems) and ozone interferences are thought to be negligible (because of low ozone concentrations).

[40] Elevated methanol and acetone were encountered in ITOP for air masses with upwind anthropogenic sources, whether transported via the middle or low level transport routes of sections 3.6 and 3.7. These two species were correlated ($R^2 = 0.57$ all data points, 0.64 excluding biomass data points) with a slope independent of anthropogenic air mass type as defined by CO (Figure 12). Higher concentrations of these two species were in general coincident with higher CO concentrations. A positive correlation also existed between other hydrocarbon anthropogenic tracers and acetone and methanol, while showing poorer correlation to acetaldehyde. Figure 13 shows the relationship between the oVOCs (methanol, acetaldehyde and acetone) and acetylene. All acetylene concentrations greater than 300 pptV are associated with biomass burning plumes, and a single slope fits all methanol, acetone and acetylene data, with the exception of these biomass burning influ-

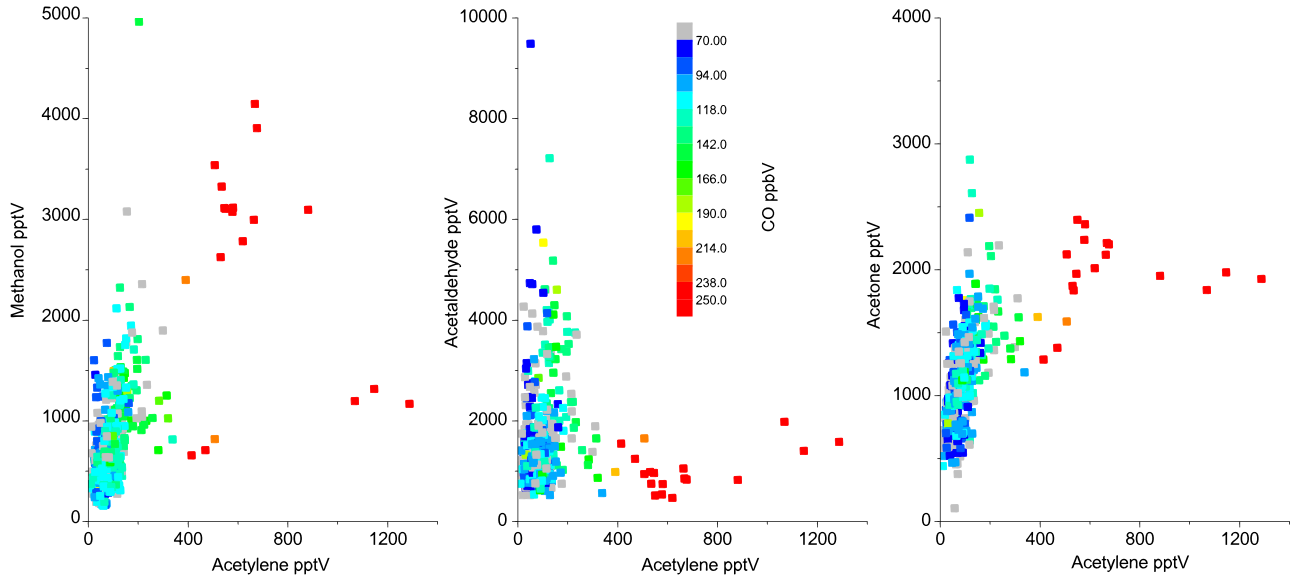

Figure 13. Methanol, acetaldehyde and acetone relationships with acetylene for all ITOP flights colored (70 to >250 ppbV) as a function of whole air sample averaged [CO]. Grey squares indicate no coincident CO data. Acetylene outliers (>300 pptV) all associated with biomass burning air mass type.

enced samples. There is some evidence therefore of elevated methanol and acetone within biomass burning plumes at concentrations beyond what is seen generally in anthropogenic outflow, but very low acetaldehyde. This would suggest some direct emission of the first two species, while the latter, which can be present downwind only through photochemical turnover of higher organics, is suppressed similar to ozone.

6. Conclusions

[41] The ITOP programme has determined that distinct chemical signatures are carried to the mid North Atlantic associated with air masses originating from a variety of geographic origins. In all cases the signatures were detected at least 1 day, and often much longer, from point of emission, and illustrate how chemical signature can be conserved over the period associated with trans Atlantic transport. The signatures were initially determined using cluster analysis without preselection of chemical criteria, and six distinct types were found to best describe the entire data set. These air mass clusters were classified on the basis of their composition and physical properties, and were found subsequently to be in very good agreement with the origins of their trajectories. The major clusters were described under the following general headings: biomass burning, low level outflow, upper level outflow, moist lower troposphere, marine and upper troposphere.

[42] Having placed observations into these clustered categories, a subsequent conclusion is that in general, the atmosphere in this remote region of the Atlantic is polluted; only the marine and upper tropospheric clusters could be described as "clean" and their back trajectories indicate in excess of 5 days (and often 10 days) since last encountering continental emissions. The chemical signatures within each air mass type appear to remain distinct over many days of atmospheric transport, and that the signature alone can be used to make a reasonable diagnosis of air mass origins in individual case study flights. In general the signatures observed were compatible with expected changes that would be brought about by chemical processing.

[43] Lower level outflow of emissions from the US continental boundary layer were significant in enhancing pollutants within both the boundary layer and lower free troposphere over the North Atlantic during summer 2004. Comparison with observations made in 1997 has illustrated that in summer 2004, some regions experienced significant elevations in O_3, NO and CO, and that this may in part be described by increased occurrence of such low level outflow. Mid and upper tropospheric transport of anthropogenic plumes were also observed within ITOP, and were linked to the passage of frontal systems over the US. The uplift of pollutants via advection associated with a warm conveyor belt to mid troposphere could be successfully simulated using RDF approaches in forecast mode enabling interceptions of such air masses. The combination of both midlevel and low level transport pathways has been used in conjunction with other aircraft observations to establish Lagrangian cases in which to study chemical transformation. The effects of boreal forest biomass burning in northern Canada and Alaska were observed on many ITOP flights and provided an additional perturbation to tropospheric composition over the comparison year of 1997. Biomass burning outflow at between 4000 and 7000 m provided on occasions very substantial elevations in CO, and hydrocarbons, and some elevation in acetone and methanol which may also have been directly emitted. The transport of significant PAN within certain biomass burning plumes was observed and there appeared a link in case studies at similar altitudes between temperature, PAN and ozone abundance. A clean marine boundary layer signature was clearly identifiable in ITOP although was elevated on occasion in longer-lived tracers such as CO likely because of the mixing to background associated with low level pollutant transport in combination with biomass burning influence throughout summer 2004.

[44] **Acknowledgments.** The authors acknowledge financial support from the United Kingdom Natural Environment Research Council (NERC), through its Upper Troposphere Lower Stratosphere thematic programme (NER/T/S/2002/00088). The authors also acknowledge the great efforts and invaluable assistance provided by staff members from the Facility for Airborne Atmospheric Measurement (FAAM), Directflight Ltd, Avalon Aero Ltd and Captains Alan Foster and Alan Roberts. Finally all members of the U.K. ITOP programme would express their appreciation of the enormous contribution made by John Reid, the FAAM Campaign Manager for ITOP, who died in May 2005.

References

Carpenter, L. J., A. C. Lewis, J. R. Hopkins, K. A. Read, M. Gallagher, and I. Longley (2004), Uptake of methanol to the North Atlantic Ocean surface, *Global Biogeochem. Cycles*, *18*, GB4027 doi:10.1029/2004GB002294.

Cook, P., et al. (2006), Forest fire plumes over the North Atlantic: p-TOMCAT model simulations with aircraft and satellite measurements from the ITOP/ICARTT campaign, *J. Geophys. Res.*, doi:10.1029/2006JD007563, in press.

Cooper, O., et al. (2006), Large upper tropospheric ozone enhancements above mid-latitude North America during summer: In situ evidence from the IONS and MOZAIC monitoring network, *J. Geophys. Res.*, *111*, D24S05, doi:10.1029/2006JD007306.

Derwent, R. G., P. G. Simmonds, S. Seuring, and C. Dimmer (1998), Observation and interpretation of the seasonal cycles in the surface concentrations of ozone and carbon monoxide at Mace Head, Ireland from 1990 to 1994, *Atmos. Environ.*, *32*(2), 145–157.

Everitt, B. S. (1993), *Cluster Analysis*, 3rd ed., Edward Arnold, London.

Fehsenfeld, F. C., M. Trainer, D. D. Parrish, A. V. Thomas, and S. A. Penkett (1996a), North Atlantic regional experiment 1993 summer intensive: Foreword, *J. Geophys. Res.*, *101*(D22), 28,869–28,875.

Fehsenfeld, F. C., P. Daum, W. R. Leaitch, M. Trainer, D. D. Parrish, and G. Hübler (1996b), Transport and processing of O_3 and O_3 precursors over the North Atlantic: An overview of the 1993 North Atlantic Regional Experiment (NARE) summer intensive, *J. Geophys. Res.*, *101*(D22), 28,877–28,891.

Fehsenfeld, F. C., et al. (2006), International consortium for atmospheric research on transport and transformation (ICARTT): North America to Europe—Overview of the 2004 summer field study, *J. Geophys. Res.*, *111*, D23S01, doi:10.1029/2006JD007829.

Heard, D. E., et al. (2005), The North Atlantic marine boundary layer experiment (NAMBLEX). Overview of the campaign held at Mace Head, Ireland, in summer 2002, *Atmos. Chem. Phys.*, *6*, 2241–2272.

Johnson, D. W., et al. (2000), An overview of the Lagrangian experiments undertaken during the North Atlantic regional Aerosol Characterisation Experiment (ACE-2), *Tellus, Ser. B*, *52*(2), 290–320.

Lewis, A. C., J. R. Hopkins, K. A. Read, L. J. Carpenter, M. J. Pilling, and J. Stanton (2005), Sources and sinks of acetaldehyde, acetone and methanol in North Atlantic marine boundary layer air, *Atmos. Chem. Phys.*, *5*, 1963–1974.

Li, Q., et al. (2002), Transatlantic transport of pollution and its effects on surface ozone in Europe and North America, *J. Geophys. Res.*, *107*(D13), 4166, doi:10.1029/2001JD001422.

Liu, H., D. J. Jacob, I. Bey, R. M. Yantosca, B. N. Duncan, and G. W. Sachse (2003), Transport pathways for Asian pollution outflow over the Pacific: Interannual and seasonal variations, *J. Geophys. Res.*, *108*(D20), 8786, doi:10.1029/2002JD003102.

Methven, J. (1997), Offline trajectories: calculation and accuracy, *Tech. Rep. 44*, U. K. Univ. Global Atmos. Modell. Program, Dep. of Meteorol., Univ. of Reading, Reading, U. K.

Methven, J., M. J. Evans, P. Simmonds, and G. Spain (2001), Estimating relationships between air mass origin and chemical composition, *J. Geophys. Res.*, *106*, 5005–5019.

Methven, J., S. R. Arnold, F. M. O'Connor, H. Barjat, K. Dewey, J. Kent, and N. Brough (2003), Estimating photochemically produced ozone throughout a domain using flight data and a Lagrangian model, *J. Geophys. Res.*, *108*(D9), 4271, doi:10.1029/2002JD002955.

Methven, J., et al. (2006), Establishing Lagrangian connections between observations within air masses crossing the Atlantic during the ICARTT experiment, *J. Geophys. Res.*, *111*, D23S62, doi:10.1029/2006JD007540.

Monks, P. S. (2000), A review of the observations and origins of the spring ozone maximum, *Atmos. Environ.*, *34*(21), 3545–3561.

Newell, R. E., V. Thouret, J. Y. N. Cho, P. Stoller, A. Marenco, and H. G. Smit (1999), Ubiquity of quasi-horizontal layers in the troposphere, *Nature*, *398*(6725), 316–319.

Olivier, J. G. J., A. F. Bouwman, C. W. M. Fandermaas, and J. J. M. Berdowski (1994), Emissions database for global atmospheric research (EDGAR), *Environ. Monit. Assess.*, *31*(1–2), 93–106.

Parrish, D. D., M. Trainer, J. S. Holloway, J. E. Yee, M. S. Warshawsky, F. C. Fehsenfeld, G. L. Forbes, and J. L. Moody (1998), Relationships between ozone and carbon monoxide at surface sites in the North Atlantic region, *J. Geophys. Res.*, *103*(D11), 13,357–13,376.

Penkett, S. A., A. Volz-Thomas, D. D. Parrish, R. E. Honrath, and F. C. Fehsenfeld (1998), Special section: North Atlantic regional experiment (NARE II): Preface, *J. Geophys. Res.*, *103*(D11), 13,353–13,355.

Penkett, S. A., et al. (2004), Long-range transport of ozone and related pollutants over the North Atlantic in spring and summer, *Atmos. Chem. Phys Disc.*, *4*, 4407–4454.

Pfister, G., P. G. Hess, L. K. Emmons, J.-F. Lamarque, C. Wiedinmyer, D. P. Edwards, G. Pétron, J. C. Gille, and G. W. Sachse (2005), Quantifying CO emissions from the 2004 Alaskan wildfires using MOPITT CO data, *Geophys. Res. Lett.*, *32*, L11809, doi:10.1029/2005GL022995.

Purvis, R. M., et al. (2003), Rapid uplift of non-methane hydrocarbons in a cold front over central Europe, *J. Geophys. Res.*, *108*(D7), 4224, doi:10.1029/2002JD002521.

Real, E., et al. (2006), Processes influencing ozone levels in Alaskan forest fire plumes during long-range transport over the North Atlantic, *J. Geophys. Res.*, doi:10.1029/2006JD007576, in press.

Reeves, C. E., et al. (2002), Potential for photochemical ozone formation in the troposphere over the North Atlantic as derived from aircraft observations during ACSOE, *J. Geophys. Res.*, *107*(D23), 4707, doi:10.1029/2002JD002415.

Singh, H. B., Y. Chen, A. Staudt, D. Jacob, D. Blake, B. Heikes, and J. Snow (2001), Evidence from the Pacific troposphere for large global sources of oxygenated organic compounds, *Nature*, *410*(6832), 1078–1081.

Stohl, A., and T. Trickl (1999), A textbook example of long-range transport: Simultaneous observation of ozone maxima of stratospheric and North American origin in the free troposphere over Europe, *J. Geophys. Res.*, *104*(D23), 30,445–30,462.

Trickl, T., O. R. Cooper, H. Eisele, P. James, R. Mücke, and A. Stohl (2003), Intercontinental transport and its influence on the ozone concentrations over central Europe: Three case studies, *J. Geophys. Res.*, *108*(D12), 8530, doi:10.1029/2002JD002735.

Val Martín, M., R. E. Honrath, R. C. Owen, G. Pfister, P. Fialho, and F. Barata (2006), Significant enhancements of nitrogen oxides, black carbon, and ozone in the North Atlantic lower free troposphere resulting from North American boreal wildfires, *J. Geophys. Res.*, *111*, D23S60, doi:10.1029/2006JD007530.

Wang, Y. H., J. A. Logan, and D. J. Jacob (1998), Global simulation of tropospheric O_3-NO_x-hydrocarbon chemistry: 2. Model evaluation and global ozone budget, *J. Geophys. Res.*, *103*(D9), 10,727–10,755.

Wenig, M., N. Spichtinger, A. Stohl, G. Held, S. Beirle, T. Wagner, B. Jähne, and U. Platt (2003), Intercontinental transport of nitrogen oxide pollution plumes, *Atmos. Chem. Phys.*, *3*, 387–393.

Wernli, H., and H. C. Davies (1997), A Lagrangian-based analysis of extratropical cyclones. 1. The method and some applications, *Q. J. R. Meteorol. Soc.*, *123*(538), 467–489.

S. R. Arnold, M. J. Evans, D. E. Heard, J. B. McQuaid, M. J. Pilling, and L. K. Whalley, Institute for Atmospheric Science, School of Earth and Environment, University of Leeds, Leeds LS2 9JT, UK. (mat@env.leeds.ac.uk)

B. J. Bandy, G. Mills, D. E. Oram, C. E. Reeves, and D. Stewart, School of Environmental Sciences, University of East Anglia, Norwich NR4 7TJ, UK.

H. Coe, J. Crosier, and P. Williams, School of Earth, Atmospheric and Environmental Sciences, Sackville Street Building, University of Manchester, Sackville Street, P.O. Box 88, Manchester M60 1QD, UK.

J. R. Hopkins, J. D. Lee, A. C. Lewis, and N. Watson, Department of Chemistry, University of York, York YO10 5DD, UK. (acl5@york.ac.uk)

J. Methven, Department of Meteorology, University of Reading, P.O. Box 243, Reading RG6 6BB, UK.

P. S. Monks and A. E. Parker, Department of Chemistry, University of Leicester, University Road, Leicester LE1 7RH, UK.

R. M. Purvis, Facility for Airborne Atmospheric Measurements, Building 125, Cranfield University, Bedford MK43 0AL, UK.